J|A|C|S
ARTICLES
Published on Web 11/08/2006

Simulating Self-Assembly of ZnS Nanoparticles into Mesoporous Materials

Dean C. Sayle,*,† Benoît C. Mangili,† Jacek Klinowski,*,‡ and Thi. X. T. Sayle†

Contribution from the DEOS, Cranfield University, Defence Academy of the United Kingdom, Shrivenham, Swindon SN6 8LA, UK, and Department of Chemistry, University of Cambridge, Lensfield Road, Cambridge CB2 1EW, UK

Received July 17, 2006; E-mail: d.c.sayle@cranfield.ac.uk; jk18@cam.ac.uk

Abstract: Characterization of materials is crucial for the quantification and prediction of their physical, chemical, and mechanical properties. However, as the complexity of a system increases, so do the challenges involved in elucidating its structure. While molecular simulation and modeling have proved invaluable as complements to experiment, such simulations now face serious challenges: new materials are being synthesized with ever increasing structural complexity, and it may soon prove impossible to generate models that are sufficiently realistic to describe them adequately. Perhaps, ultimately, it will only be possible to generate such models by simulating the synthetic process itself. Here, we attempt such a strategy to generate full atomistic models for mesoporous molecular sieves. As in experiment, this is done by allowing nanoparticles to self-assemble at high temperature to form an amorphous mesoporous framework. The temperature is then reduced, and the system is allowed to crystallize. Animations of atomic trajectories, available as Supporting Information, reveal the evolution of multiple seeds which propagate to form a complex framework. The products are polycrystalline mesoporous framework structures containing cavities connected by channels running along "zero", one, two, and three perpendicular directions. We suggest that it is easier to generate these model structures by attempting to simulate the synthetic process rather than by using more conventional techniques. The strategy is illustrated using ZnS as a model system. Further development of the mathematics of minimal surfaces will advance our understanding of these structures.

Introduction

Frameworks of mesoporous molecular sieves accommodate internal channels and cavities.[1] They are important technologically with applications in catalysis,[2] separation technology, ion exchange, sensors, etc.[3] An important class is the zeolites, which comprise periodic arrays of channels and cavities of molecular dimensions, enabling them to be used as shape-selective catalysts. However, in contrast to many catalysts in which the chemistry occurs on the external surfaces, catalysis in zeolites occurs within a channel or cavity facilitating shape and size selectivity.[4]

Zeolitic structures are complex, and therefore atomistic models have been constructed by extracting atom positions from XRD data. Computational visualization tools are used extensively to help us understand more easily the complex three-dimensional zeolitic framework structure. Moreover, in addition to structural characterization, atomistic simulation has enabled people to explore and predict the chemical properties of these microporous materials.[5]

It has been suggested[2] that internal channels and cavities of mesoporous materials, such as zeolites, offer the promise of "nanosized chemical laboratories," and considerable efforts have been focused on the design and synthesis of various framework structures.[6] The ultimate goal is to be able to use inorganic framework structures to mimic enzymatic processes.

Many experimental approaches to the synthesis of framework structures have explored the use of templates. For example, Li et al.[1] synthesized mesoporous metal oxides with ordered mesopores using nanocrystals as the building block, held together by an amorphous "glue". A different strategy was employed by Roggenbuck and Tiemann who used a carbon exotemplate to synthesize thermally stable MgO containing a periodic array of pores 4−8 nm in diameter.[7] Zou et al.[8] synthesized a chiral mesoporous germanium oxide with a primitive cell volume of 67 640 Å^3 and crystalline pore walls. This raised the possibility of fabricating an enantiopure material using chiral templates, a step closer to enzymatic mimicry. A review of templating methods for the preparation of porous

† Cranfield University.
‡ University of Cambridge.

(1) Li, D. L.; Zhou, H. S.; Honma, I. *Nat. Mater.* **2004**, *3*, 65−72.
(2) Thomas, J. M.; Catlow, C. R. A.; Sankar, G. *Chem. Commun.* **2002**, 2921−2925.
(3) Férey, G. *Science* **2001**, *291*, 994−995.
(4) Foster, M. D.; Simperler, A.; Bell, R. G.; Delgado Friedrichs, O.; Almeida Paz, F. A.; Klinowski, J. *Nat. Mater.* **2004**, *3*, 234−238.
(5) To, J.; Sokol, A. A.; French, S. A.; Catlow, C. R. A.; Sherwood, P.; van Dam, H. J. J. *Angew. Chem., Int. Ed.* **2006**, *45*, 1633−1638.
(6) Huang, L. M.; Wang, Z. B.; Sun, J. Y.; Miao, L.; Li, Q. Z.; Yan, Y. S.; Zhao, D. Y. *J. Am. Chem. Soc.* **2000**, *122*, 3530−3531.
(7) Roggenbuck, J.; Tiemann, M. *J. Am. Chem. Soc.* **2005**, *127*, 1096−1097.
(8) Zou, X. D.; Conradsson, T.; Klingstedt, M.; Dadachov, M. S.; O'Keeffe, M. *Nature* **2005**, *437*, 716−719.

structures with prescribed structural, surface, and morphological properties is available.[9]

The success that atomistic simulation has had in exploring and predicting the structure and properties of zeolites is well documented,[4,10,11] and it is therefore desirable to continue to use simulation to help complement experiment in the study of other mesoporous systems. However, there are several challenges which need to be addressed before constructing realistic models. For example, we need to know the atomistic detail of the crystal structure of the framework, the size, shape, and curvature of the channels and cavities, as well as their connectivity. Microstructural detail is also important. In particular, it is unusual[12] to obtain single crystals of mesoporous materials, and most samples are available as microcrystalline powders. The atomistic model must therefore include misoriented grains, together with the associated grain boundaries and grain junctions. The morphology of the curved surfaces also needs to be defined, a somewhat daunting prospect. In particular, it may prove disingenuous to generate such complex models using conventional simulation approaches. Accordingly, we have taken an easier approach and one that is similar to experiment, in that we generate the nanoporous materials via the self-assembly of nanoparticles.

We have taken ZnS as a trial system for which experimental data are available to help validate our models. For example, Scholz et al. fabricated mesoporous ZnS using ZnS nanocrystallites,[13] and Hu et al. made mesoporous ZnS nanoparticles 60 nm in diameter via the self-assembly of ZnS nanocrystal building blocks 3−4 nm in size.[14] The resulting material had a surface area as high as 156 m^2/g. Rana et al. used an ultrasound-mediated method to prepare stable mesoporous ZnS networks using ZnS nanoparticles,[15] returning surface areas of 210 m^2/g and average pore diameters of 28 Å. HRTEM analysis revealed a mesostructure consisting of closely spaced ZnS nanocrystallites ca. 3 nm in size.

Methods

In this section we discuss the potential models used to describe the interactions between Zn and S, the simulation code used to perform the molecular dynamics (MD) simulations, and our strategy for generating mesoporous ZnS via the self-assembly of ZnS nanoparticles.

Potential Models and Simulation Code. ZnS is described using the Born model of an ionic solid of the form

$$U_{ij} = \frac{Q_i Q_j}{r_{ij}} + A \exp\left[-\frac{r_{ij}}{\rho}\right] - C r_{ij}^{-6} \qquad (1)$$

where Q is the charge of the ions I and j, r is the interionic distance, and A and C are parameters which are fitted to the structure and properties of ZnS. For highly ionic materials, this form works well in describing the structure and properties. However, for partially covalent materials such as ZnS, additional functions are introduced to help describe the directionality of the structure. We have used a three-body potential

$$U(\Theta) = \frac{k}{2}(\theta - \theta_o)^2 \times \exp\left[\frac{-(r_{ij}^8 + r_{ik}^8)}{\sigma^8}\right] \qquad (2)$$

where k is the force constant and θ_o is the equilibrium bond distance. Preliminary tests using this potential revealed the need to introduce an exponential decay to the potential to smooth the discontinuity between ions moving between coordination shells. The potential parameters, including the exponential decay, are given in Table 1. These parameters were taken from refs 16 and 17 and have been successfully used to describe the crystal structure, elastic and dielectric properties of ZnS (both the wurtzite and sphalerite structures), its defect properties,[16] the structure of its surfaces,[17] nanobubbles[18] and nanocrystals,[19] embryonic growth in solution,[20] and water-driven structural transformations.[21] Accordingly, we expect these potentials to be well suited to explore the crystallization and structure of mesoporous ZnS. The DL_POLY code,[22] which imposes 3D periodic boundary conditions, was used to perform all the molecular dynamics simulations. Further details of this approach can be found elsewhere.[23]

Table 1. Potential Parameters Used to Describe ZnS

	Buckingham short-range parameters (eq 1)			
species	A (eV)	ρ (Å)	C (eV Å^6)	cutoff (Å)
Zn−S	613.356	0.3999	0.0	10.0
S−S	1200.0	0.149	120.0	10.0
	three-body parameters (eq 2)			
	k (eV rad^{-2})	θ_o (deg)	σ (Å)	cutoff (Å)
S−Zn−S	0.713	109.47	3.0	4.0
	shell model parameters			
	mass	charge (e)	k_1 (eV Å^{-2})	
S_{core}	30.0	1.357		
S_{shell}	2.0	−3.357	27.69	
Zn	65.0	2.0		

Self-Assembly Strategy. We describe our simulation approach using schematics (Figure 1). An amorphous/molten ZnS nanoparticle, comprising 25 200 atoms, is placed in the center of a simulation cell (Figure 1a). The figure also shows nanoparticles in neighboring cells, which are periodic images of the central nanoparticle. The interactions between the nanoparticle and its images will increase as the size of the simulation cell is reduced (Figure 1b). Eventually, under MD simulation, the nanoparticle will aggregate with its neighbors (Figure 1c), resulting in a simulation cell (Figure 1d). Periodic arrays of these shapes clearly give rise to a periodic array of holes or channels in three dimensions (Figure 1e,f).

We can influence the size of the channels in a particular direction by changing the size (x,y,z) of the simulation cell. For example, if we

(9) Zhao, X. S.; Su, F. B.; Yan, Q. F.; Guo, W. P.; Bao, X. Y.; Lv, L.; Zhou, Z. C. *J. Mater. Chem.* **2006**, *16*, 637−648.
(10) Delgado Friedrichs, O.; Dress, A. W. M.; Huson, D. H.; Klinowski, J.; Mackay, A. L. *Nature* **1999**, *400*, 644−647.
(11) Lewis, D. W.; Willock, D. J.; Catlow, C. R. A.; Thomas, J. M.; Hutchings, G. J. *Nature* **1996**, *382*, 604−606.
(12) Hetherington, N. B. J.; Kulak, A. N.; Sheard, K.; Meldrum, F. C. *Langmuir* **2006**, *22*, 1955−1958.
(13) Scholz, S. M.; Vacassy, R.; Lemaire, L.; Dutta, J.; Hofmann, H. *Appl. Organomet. Chem.* **1998**, *12*, 327−335.
(14) Hu, J. S.; Ren, L. L.; Guo, Y. G.; Liang, H. P.; Cao, A. M.; Wan, L. J.; Bai, C. L. *Angew. Chem., Int. Ed.* **2005**, *44*, 1269−1273.
(15) Rana, R. K.; Zhang, L. Z.; Yu, J. C.; Mastai, Y.; Gedanken, A. *Langmuir* **2003**, *19*, 5904−5911.
(16) Wright, K.; Jackson, R. A. *J. Mater. Chem.* **1995**, *5*, 2037−2040.
(17) Hamad, S.; Cristol, S.; Catlow, C. R. A. *J. Phys. Chem.* **2002**, *B106*, 11002−11008.
(18) Hamad, S.; Catlow, C. R. A.; Spano, E.; Matxain, J. M.; Ugalde, J. M. *J. Phys. Chem.* **2005**, *B109*, 2703−2709.
(19) Zhang, H. Z.; Huang, F.; Gilbert, B.; Banfield, J. F. *J. Phys. Chem.* **2003**, *B107*, 13051−13060.
(20) Hamad, S.; Cristol, S.; Catlow, C. R. A. *J. Am. Chem. Soc.* **2005**, *127*, 2580−2590.
(21) Zhang, H. Z.; Gilbert, B.; Huang, F.; Banfield, J. F. *Nature* **2003**, *424*, 1025−1029.
(22) Smith, W.; Forester T. R. DL_POLY. A parallel molecular dynamics simulation package developed at Daresbury Laboratory under the auspices of the Engineering and Physical Sciences Research Council (EPSRC) for the EPSRC's Collaborative Computational Project for the Computer Simulation of Condensed Phases (CCP5) and the Advanced Research Computing Group (ARCG) at Daresbury Laboratory. http://www.dl.ac.uk/TCSC/Software/DLPOLY. 1996.
(23) Sayle, T. X. T.; Catlow, C. R. A.; Maphanga, R. R.; Ngoepe, P. E.; Sayle, D. C. *J. Am. Chem. Soc.* **2005**, *127*, 12828−12837.

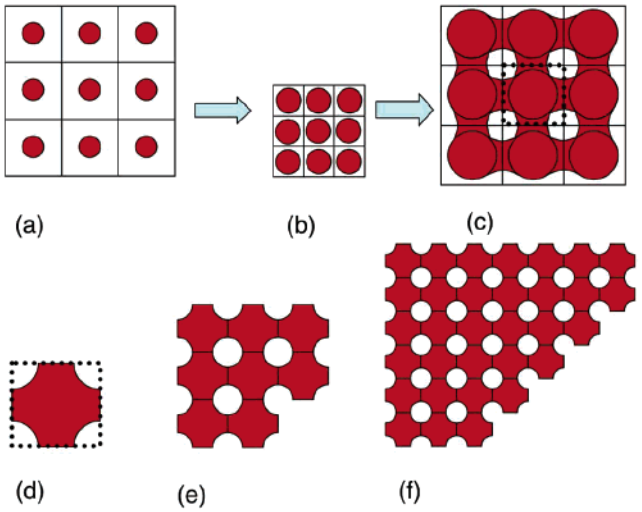

Figure 1. Generation of an atomistic model for a mesoporous material. (a) A nanoparticle within a simulation cell surrounded by its eight periodic images; (b) same as (a) but with a reduced simulation cell size; (c) aggregation of the nanoparticle with its periodic images; (d) structure of the nanoparticle taken from (c); (e) periodic arrays of (d) facilitating the channels; (f) larger array.

increase *x* and *z*, then a channel (along *y*) with a larger diameter would result. Similarly, by reducing *x* and *z*, a smaller channel would evolve. If *x* and *z* are reduced in different proportions, a channel with an elliptical cross-section will result. Ultimately, a channel can be blocked by sufficient reduction in size of the simulation cell. We can therefore generate channels that traverse one, two, and three perpendicular directions. If we were to block all the channels, a periodic array of cavities will evolve with no connectivity between them. This strategy was used to generate channels in "zero", one, two, and three directions. In the following section we describe in more detail the formation of a 2D channel network.

That the structure of the uniform mesoporous material can be represented by just a single nanoparticle may appear somewhat abstract and artificial, because the nanoparticle is necessarily influenced "by itself." It would clearly be more satisfying to have real nanoparticles as neighbors as opposed to images. We expect that this would yield similar and more realistic structures, but as the nanoparticle comprises 25 200 atoms, this would at present prove computationally prohibitive. Moreover, this is not required by the symmetry of the system: what is needed is the irreducible representation, which is a *single* nanoparticle. Our approach is therefore to use a single nanoparticle but one that comprises as many ions as can be accommodated within the computational facilities available. This approach enables the framework walls, channels, and cavities to be as large as possible.

Evolution of Channels. A nanoparticle of ZnS with rock salt structure $28 \times 30 \times 30 = 25\,200$ atoms in size was constructed and placed inside a simulation cell of size $10 \times 10 \times 10$ nm^3. We note that the initial rocksalt crystal structure of the nanoparticle is not important because the nanoparticle will lose all structure after it has been amorphised. The Zn−S interionic distances were set to 4 Å, and MD simulation was performed for 467 ps at 3000 K. Snapshots taken during the MD simulation are shown in Figure 2 (where multiple simulation cells have been used to show the evolution of the periodic channels).

In Figure 2a, the system is shown after 10 ps of MD simulation and reveals the initial amorphization and partial sphericalisation of the nanoparticle. Under further MD, the nanoparticle starts to aggregate with its periodic images and, after 20 ps, a channel perpendicular to the surface plane evolves, Figure 2b. After 110 ps, a more spherical channel is evident as the system attempts to minimize its surface energy, Figure 2c. Similar images in perpendicular directions to that shown in Figure 2a−c are shown in Figure 2d−f and 2g−i. Clearly, in Figure 2g−i, the size of the simulation cell is sufficiently small that the channel, which evolves initially (Figure 2h), is eventually blocked (Figure 2i).

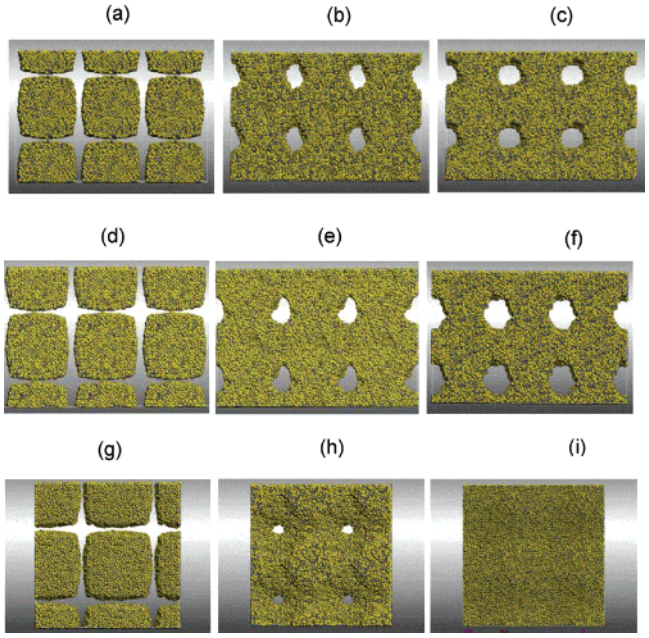

Figure 2. Snapshots of the ZnS atom positions, taken during the MD simulation, showing the evolution of the channel network; (a−c), (d−f), and (g−i) show views in three perpendicular directions. Supercells are depicted to reveal the channels: (a−c) and (d−f) show a 3×2 supercell, and (g−i), a 2×2 supercell. (a) After 10 ps of MD simulation revealing the amorphous/molten structure of the nanoparticle; (b) after 20 ps of MD showing the aggregation of the nanoparticle with its periodic images to reveal pseudo-elliptical channels; (c) after 110 ps revealing spherical channels. (d) 10 ps; (e) 20 ps; (f) 110 ps. (g) 10 ps; (h) 70 ps; (i) 110 ps — here the channels have closed up completely. The figures use a sphere model representation of the atom positions: Zn is blue and S is yellow.

Crystallization. Thus far the simulation has resulted in the formation of an amorphous/molten mesoporous material with channels in 2D. The next step is to crystallize the ZnS, which is achieved by reducing the temperature to below the melting point: constant volume MD simulation was performed at a temperature of 1500 K for 1895 ps. Finally, the system is cooled by performing MD simulation at 1 K for 100 ps followed by shell-model MD at 1 K for 50 ps. The latter, low-temperature simulation acts effectively as an energy minimization.

Molecular graphics were used to analyze the atom trajectories during the MD simulations, and animations of the crystallization were made (three have been deposited as Supporting Information). Snapshots of one particular region, taken during the crystallization of the 2D system, are presented in Figure 3a−l. The final structure is shown in Figure 4, which depicts a supercell ($2 \times 4 \times 4$ unit cells) to show more clearly the interconnecting 2D channel system; Zn ions are not shown for clarity. Mesoporous structures with 0-, 1-, and 3D channel systems were constructed in a fashion similar to that of the 2D system, by changing the simulation cell size. Details are given in Table 2.

Results

In this section, we discuss the crystallization of the framework in detail for the 2D system, the final low-temperature structures and channel systems for the 0-, 1-, 2-, and 3D systems, and the crystal structure of the framework and surfaces exposed at the channels.

Crystallization. Figure 3 shows snapshots of the crystallization of a small segment for the 2D system. After 5 ps of MD simulation, the structure appears amorphous (Figure 3a). Watching animations of the crystallization (see Supporting Informa-

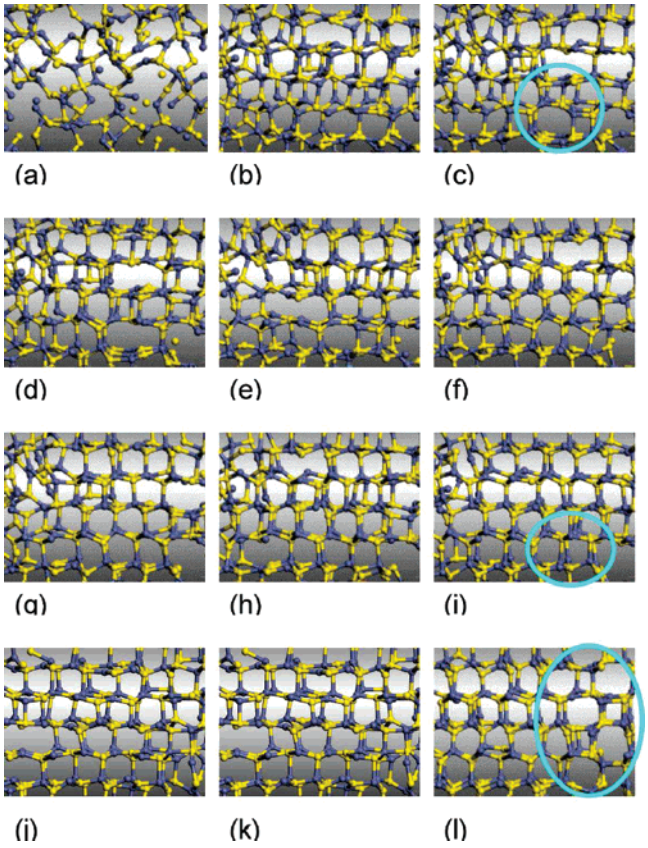

Figure 3. Snapshots taken during the MD simulation of the 2D system showing the crystallization of the ZnS; ball-and-stick model representations of the Zn (blue) and S (yellow) atom positions. (a) After 5 ps showing the amorphous/molten ZnS; (b) after 500 ps revealing the (partial) crystallization of the ZnS; (c) after 700 ps, the area circled accommodates a 4−8-membered ring structure; (d) 750 ps; (e) 800 ps; (f) 850 ps; (g) 900 ps; (h) 950 ps; (i) 1000 ps — the region highlighted by the blue circle has now rearranged into a wurtzite structure; (j) 1250 ps; (k) 1500 ps; (l) 1895 ps — the region highlighted has returned to a 4−8-membered ring conformation.

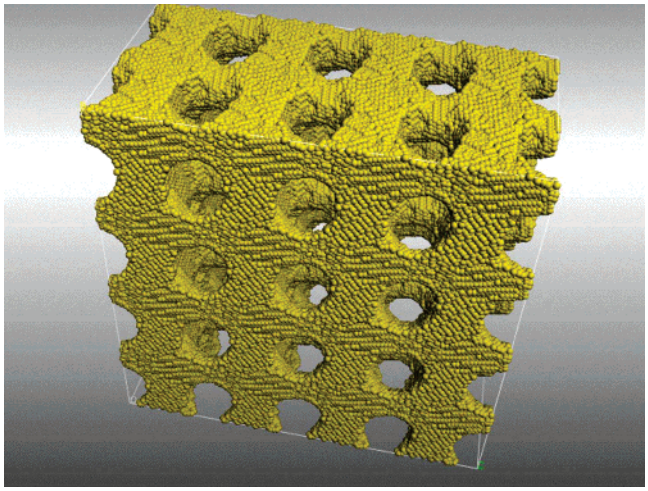

Figure 4. Final low-temperature (1 K) sphere model representation of the mesoporous model with 2D channels. A 2 × 4 × 4 supercell is shown with only the S ions (yellow) shown to help improve the clarity of the figure.

tion) reveals that initially several crystalline seeds evolve.[23,24] These have alternating (−Zn−S−Zn−S−Zn−S−) six-membered ring structures with chair and boat conformations. During the crystallization Zn and S ions appear to condense onto the outer surface of the crystalline seeds, propagating their structure. As the crystalline regions evolve, they impinge upon other crystalline regions, resulting in the formation of grain boundaries. This is because the crystalline seeds evolve in different orientations with respect to each other.

A crystalline region that has evolved after 500 ps is shown in Figure 3b, revealing the hexagonal structure. These hexagonal rings are transient: they evolve and rearrange by connecting to other six-membered rings. In particular, after 700 ps (Figure 3c), a four-membered ring is seen to have evolved and is connected to an eight-membered ring (the region is circled in the figure). We note that four-membered rings have been observed by Hamad et al., who explored the embryonic stages of crystallization in ZnS.[18] After 1000 ps (Figure 3i), the four- and eight-membered rings have disbanded, and a six-membered ring structure returns. Finally, after 1895 ps, the four- and eight-membered rings have reformed (Figure 3l). We note that, on side profile, the 4−8-membered ring structures are hexagonal rings.

Analysis of the structure using molecular graphics reveals that the six-membered rings have the wurtzite structure, which is a high-temperature form of ZnS,[25] although some studies have shown that, even at low temperatures, small nanocrystallites can accommodate the wurtzite structure.[26] We might have expected the sphalerite structure to evolve, which is a common low-temperature form of ZnS. However, we did not see evidence for domains accommodating this structure.

Low-Temperature Structures. The final low-temperature structure of the 2D system is shown in Figure 4. A supercell (2 × 4 × 4) clearly shows the interconnecting 2D channels. The primitive unit cell of the 2D system is shown in Figure 5. The bottom half of the structure has been depicted using spheres to represent the Zn and S atom positions, while the top part of the figure has been surface rendered. The latter is to show that the mesoporous framework comprises many interconnecting grains separated by (general) grain boundaries and grain junctions; the different misoriented grains are colored to aid visualization. The atomistic (ball-and-stick representation) structure of one of the pillars is shown in Figure 5b.

The surface structure of the 2D system is shown in Figure 6a, essentially the top of the structure has been "sliced off" to show the channels and cavities more clearly. Inspection of the figure reveals that the channel and cavity surfaces exhibit high two-dimensional curvature, and therefore assigning a particular Miller index to the facets exposed is perhaps disingenuous. The curvature of the channel is clearer in Figure 6b, which reveals that the channel accommodates an elliptical, rather than spherical, structure.

Part of a channel corresponding to the 1D system is shown in Figure 6c. Here we can easily see the wurtzite structure (left), which appears to expose the (001) surface at the channel wall. However, this surface is curved ("zigzag") in a direction along the channel, and therefore assignation of this Miller index is perhaps misleading. In particular, the chemistry that we might expect of a ZnS (001) wurtzite surface is unlikely to be reflected at this channel because of the high curvature. On the other hand,

(24) Lu, D.; Katou, T.; Uchida, M.; Kondo, J. N.; Domen, K. *Chem. Mater.* **2005**, *17*, 632−637.
(25) Huang, F.; Banfield, J. F. *J. Am. Chem. Soc.* **2005**, *127*, 4523−4529.
(26) Zhao, Y. W.; Zhang, Y.; Zhu, H.; Hadjipianayis, G. C.; Xiao, J. Q. *J. Am. Chem. Soc.* **2004**, *126*, 6874−6875.

Table 2. Simulation Details Used to Generate Mesoporous ZnS with 0D, 1D, 2D, and 3D Channels

	simulation cell size (Å)			molecular dynamics simulations			
cavity connectivity	*x*	*y*	*z*	3000 K rigid ion, ps	1500 K rigid ion, ps	1 K rigid ion, ps	1 K shell, ps
0D	90	90	90	200	2060	100	63
1D	85	105	105	30	2245	100	85
2D	100	100	100	467	1895	100	50
3D	100	106	106	50	2000	250	50

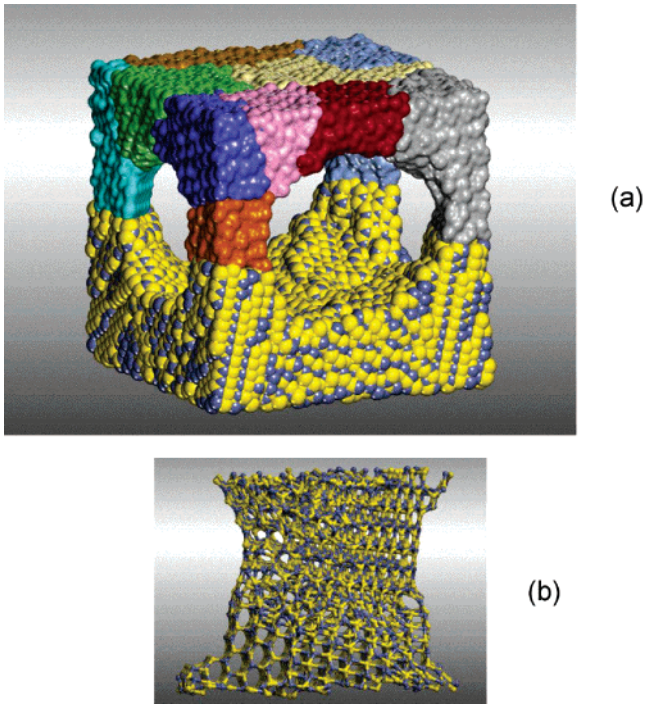

Figure 5. (a) Primitive simulation cell of the mesoporous model with 2D channels; the final low temperature (1 K) structure is shown. The bottom half of the figure is a sphere model representation of the Zn (blue) and S (yellow) ion positions, and the top half is surface rendered with various colors to differentiate the misoriented ZnS grains; (b) shows one of the pillars, cut from (a), using a ball-and-stick representation of the atom positions.

the curvature is not continuous. It must necessarily be resolved only down to the atomistic level; rather we are observing regions of faceting.

The crystal structure of various parts of the framework (2D system) is shown in Figure 7. The atomistic structure of a region, which conforms to the wurtzite structure, is given in Figure 7a, and a region, comprising four- and eight-membered rings, in Figure 7b. In Figure 7c the wurtzite structure can be adjudged to comprise hexagons accommodating a chair conformation, whereas conversely, in the four- and eight-membered ring structure, Figure 7d, the hexagons conform to a "boatlike" structure. A region that comprises both types of structure is shown in Figure 7e.

Figures 8−11 show the structure of the mesoporous ZnS materials with 0-, 1-, 2-, and 3D structures with surface rendering to depict the accessible surfaces, channels, and cavities. Calculated surface areas, pore diameters, cell volumes, and densities are given in Table 3. Clearly, the 0D system has no "channels," and therefore the cavities are not connected.

Discussion

In the following sections we compare our simulations with a study that explores the crystallization of real mesoporous

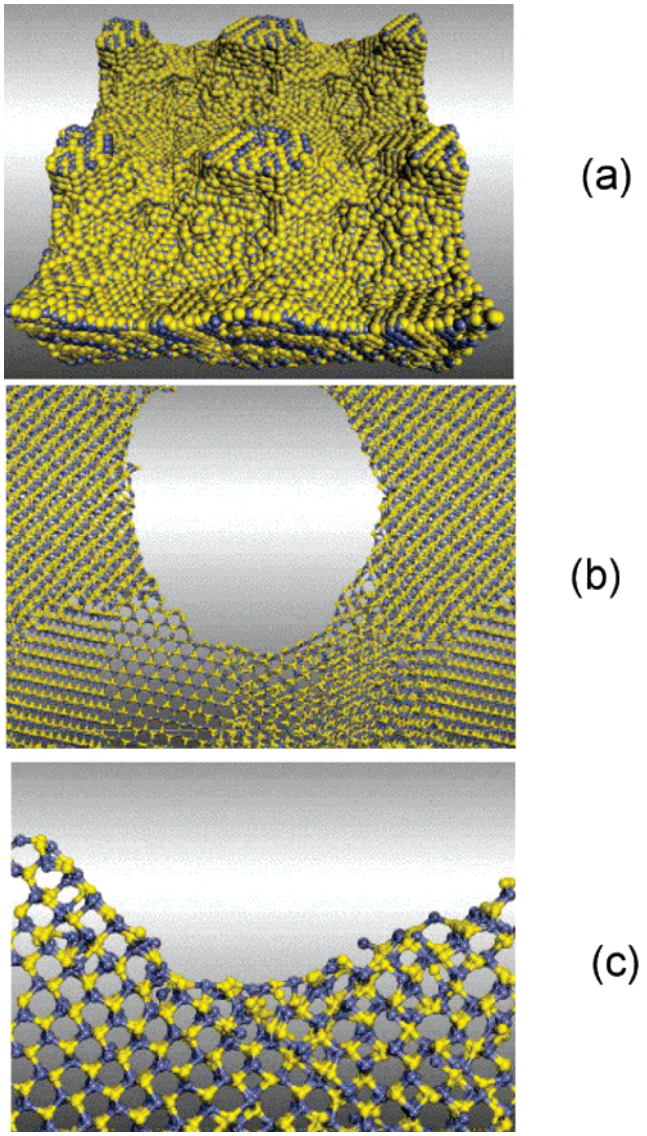

Figure 6. (a) Sphere model representation of the atom positions, Zn (blue) and S (yellow), of the 2D system. A 2 × 2 × 1 supercell is depicted with the "top" sliced off to show more clearly the surface structure of the channels and cavities within this framework structure. (b) A view looking through one of the channels in the 2D system revealing the high curvature of the elliptical channel; various grain boundaries and grain junctions are evident in the figure — ball-and-stick model representation. (c) Ball-and-stick model representation of the 1D system, viewing along one of the channels.

materials observed using TEM. This is followed by a discussion and possible rationale underlying the evolution of wurtzite and 4−8-membered ring structures. Finally, we raise the possibility of classifying the mesoporous framework structures as minimal surfaces, which is potentially very important. In particular, we argue that it may be possible to predict catalytic properties by describing the surface mathematically as a continuous function.

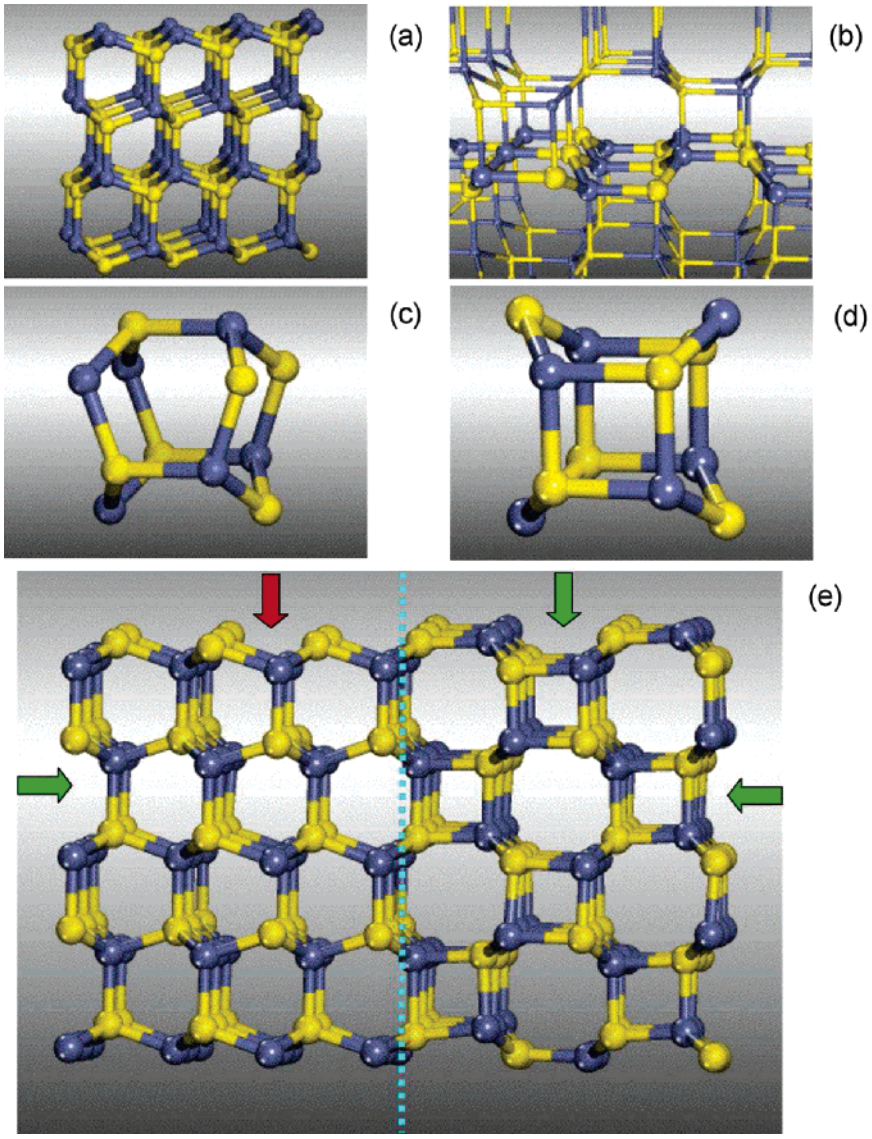

Figure 7. Ball-and-stick model representation of the Zn (blue) and S (yellow) atom positions comprising the 2D system. (a) Region conforming to the wurtzite structure; (b) region conforming to the "4−8-membered ring structure"; (c) segment of the wurtzite structure showing the hexagons in a chair conformation; (d) segment of the "4−8-membered ring" structure where the hexagons accommodate a boat conformation; (e) region comprising both the wurtzite and "4−8-membered ring" structure, with the green arrows indicating type-I surfaces which have no dipole and the red arrow indicating a "type-III" surface, which is associated with a surface dipole. Note this segment has been cleaved from the 2D system, and the surfaces indicated by the arrows are hypothetical; they are not exposed at the surfaces of the channels or cavities.

Observing Crystallization via TEM. Lu et al. used transmission electron microscopy (TEM) to observe the crystallization of mixed metal oxide mesoporous materials starting from amorphous precursors.[24] They generated Nb−Ta and Mg−Ta oxides with mean pore sizes of ca. 5 nm, wall thicknesses of 3 nm, and surface areas of ca. 200 $m^2\ g^{-1}$.

Experimentally, in a vacuum, crystallization was determined to be highly localized and led to the formation of a polycrystalline structure which retained the original pore size. Conversely, in air, crystallization resulted in single crystals, hundreds of nanometers in diameter. The authors tentatively attributed this difference to the presence or absence of air. Moreover, they proposed a mechanism explaining the single-crystalline and polycrystalline structures. In particular, they argued that "oxygen exchange (in air) promotes the long-range mobility of the metal ions: mass transfer occurs over a large region and the (original) small mesopores merge into larger mesopores to minimize the total surface energy".

In the present study, by watching the crystallization animations (Figure 3 and Supporting Information) we observe, similar to experiment, the evolution of many localized crystalline seeds leading to the formation of a polycrystalline mesoporous structure. Our simulations support the idea of the highly localized crystallization proposed in the experimental study. Simulation and modeling are therefore valuable complementary techniques which can provide realistic crystallization and structural details of highly complex mesoporous systems with full atomistic resolution.

We note that our simulated crystallization occurs over nanosecond time scales and is therefore faster than that observed experimentally. We are thus aware of the possibility that the fast crystallization may influence the structure of the atomistic models generated using this technique.

Crystal Structures. The "4−8-membered ring" structure which is part of the ZnS-based mesoporous materials has the

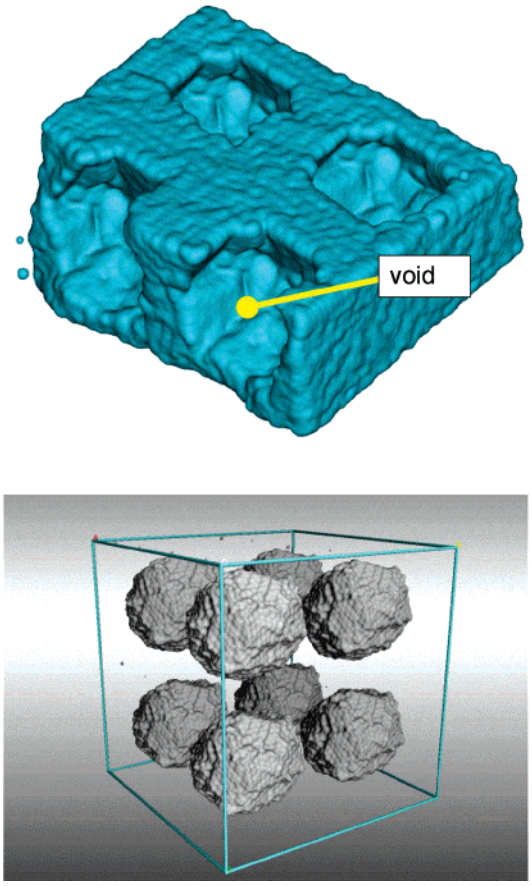

Figure 8. "0D" mesoporous framework structure. (Top) Surface rendered model (2 × 2 supercell shown); (bottom) representation showing only the (internal) surface (2 × 2 × 2 supercell). We note that there are no channels, and therefore the cavities are not connected.

same crystal structure as zeolite BCT. Therefore, in accordance with Hamad and Catlow[27] we refer to this structure as the BCT phase.

ZnS has two structural polymorphs: wurtzite (hexagonal) and sphalerite (cubic), and therefore two surprising issues emerge from our results: first, no sphalerite has evolved and, second, the evolution of extended regions which conform to the BCT phase. Extended arguments concerning this question can be found in the Supporting Information. Specifically, we explore structural changes as a function of (nano)size and environment, the influence of the internal surfaces, the energetics of phase ordering as determined by the potential model, and the high speed of crystallization.

Minimal Surfaces. Inspection of the amorphous/molten structures for each of the four systems suggests that they may be described in terms of minimal surfaces. D'Arcy Thompson, author of the classic book "On Shape and Form", first published almost a century ago, famously observed that "shape determines function."[28] The crucial step in the recent advance in structural chemistry, from classical geometry to three-dimensional differential geometry, has been the use of curved surfaces in describing an astonishing variety of structures and properties.[29]

The key concept of curvature, originally developed by Newton using the term "crookedness", is as follows: The arc length along a planar curve is related to the tangent to the curve. The curvature at a particular point on the curve is defined as the limit of the tangent as the arc length approaches zero at that point. *Mean curvature* is the arithmetic mean of the curvature of a surface at two mutually orthogonal directions.

(27) Hamad, S.; Catlow, C. R. A. *J. Cryst. Growth* **2006**, in press.
(28) Thompson, D. A. *On Growth and Form*, 2nd ed.; Cambridge University Press: Cambridge, 1968.
(29) von Schnering, H. G.; Nesper, R. *Angew. Chem., Int. Ed. Engl.* **1987**, *26*, 1059−1080.

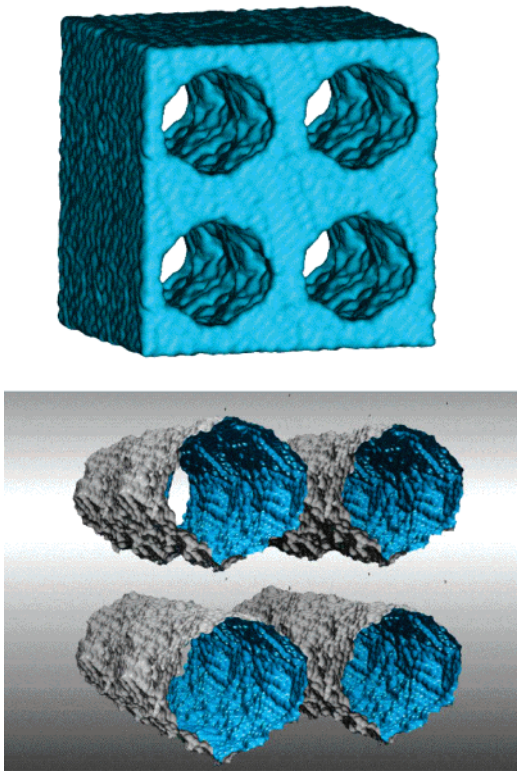

Figure 9. "1D" mesoporous framework structure. (Top) Surface rendered model (2 × 2 × 2 supercell); (bottom) representation showing only the surface (2 × 2 × 2 supercell) exposed at the channels and cavities.

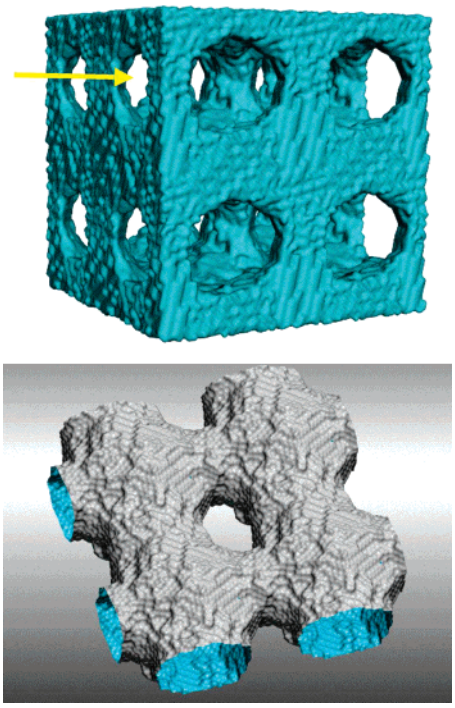

Figure 10. "2D" mesoporous framework structure. (Top) Surface rendered model (2 × 2 × 2 supercell shown); (bottom) representation showing only the surface (2 × 2 × 1 supercell).

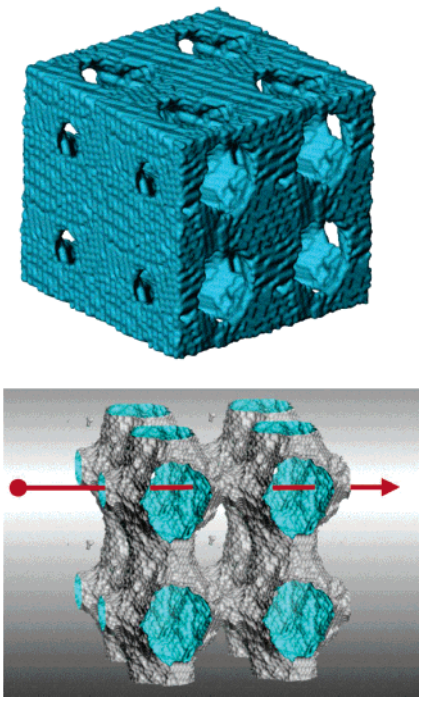

Figure 11. "3D" mesoporous framework structure. (Top) Surface rendered model (2 × 2 × 2 supercell shown); (bottom) representation showing only the surface (2 × 2 × 2 supercell).

Table 3. Attributes Associated with Mesoporous ZnS[a]

cavity connectivity	density (g/cm³)	surface area (m²/g)	surface energy J/m²	pore size (nm)	surfaces exposed
0D	2.80	391	4.5	6.5 (cavity)	{001}
1D	2.18	377	3.9	7.1	{001}
2D	2.05	406	4.6	5.7 × 7.5; 5.0 × 5.0	
3D	1.82	362	4.1	5.7 × 5.7; 7.2 × 6.5; 4.0 × 4.5	

[a] Approximate surface areas were calculated using a "solvent accessible surface" approach with a solvent molecule with a radius of 2 Å.

When a wire frame is dipped into soapy water, a thin film is formed. Surface tension minimizes the energy of the film, which is proportional to its surface area. The film thus has the smallest area consistent with the shape of the frame and with the requirement that the *mean curvature of the film be zero at every point.* This is a minimal surface. Minimal surfaces which are periodic in three independent directions are of special interest, because atoms in a variety of seemingly unconnected structures such as cristobalite, quartz and numerous zeolites,[30,31] diamond, cutting steel, bicontinuous polymer mixtures, lyotropic colloids, detergent films, lipid bilayers, starch, and biological formations lie on such surfaces. Self-assembled colloid structures are templates in the inorganic and organic polymerization reactions which lead to mesoporous molecular sieves.[32,33] Such surfaces are thus of interest, not only to the structural chemist but also to the biologist, structural engineer, and materials scientist. A full discussion of minimal surfaces can be found in refs 34 and 35. Figures 1c and 2 show the evolution of the P minimal surface (known as "the plumber's nightmare")[35] as the molten nanoparticles aggregate. This is not surprising considering the presence of surface forces in the molten phase. Figure 12a shows a primitive cell of the 3D system at the start of the crystallization step. The structure clearly forms the P minimal surface (Figure 12b).[36] As the atomistic system crystallizes at temperatures lower than the melting point, the interactions between the ions are minimized under molecular dynamics simulation. The ions move into a low-energy configuration, and planar facets are seen to evolve. A further deviation (compared with the molten system) from the perfect minimal surface, Figure 12b, then appears. Figure 12c shows the final crystallized structure.

The structures of mesoporous materials such as ZnS have important implications for their chemical and electronic properties (i.e., catalysis, sensors, optical, visible light absorption in chemical cleavage of bonds). For example, the strain within the mesoporous crystalline lattice will likely be different from analogous nanocrystals or the bulk parent material, because of the curvature of the "channel-cavity-pillar" architecture and thin walls. For example, in a nanocrystal, the surface may be considered as convex, while, in the mesoporous analogue, the surface is concave.

Conclusions

We describe full atomistic models of the polycrystalline mesoporous ZnS framework structures. To generate these models we have attempted to simulate experimental synthetic processes. The framework was generated by allowing amorphous/molten nanoparticles of ZnS to self-assemble under high-temperature MD simulation, which resulted in the formation of a periodic array of cavities interconnected by channels traversing "zero", one, two, and three perpendicular directions.

The resulting amorphous mesoporous frameworks were crystallized by allowing the system to cool, and long-duration MD simulations were performed at reduced temperatures. Animations of the atom trajectories during the MD simulation revealed the evolution of many localized crystalline seeds, which grew in size as (amorphous) ions condensed onto their surface. Eventually, the crystallization fronts, emanating from the individual (misoriented) seeds, impinged upon each other, resulting in the evolution of a polycrystalline framework, comprising a plethora of grain boundaries and grain junctions which separate the individual grains.

The crystallization is similar to that reported by Lu et al. for metal-oxide-based mesoporous materials.[24] They concluded that "highly localized crystallization led to the formation of a polycrystalline mesoporous framework structure that retained the original pore size". We note that Lu et al. infer this crystallization behavior, based upon their final structures, rather than having "observed" it. Here, we provide movies depicting such crystallization (with atomistic detail), which are available as Supporting Information. It is unlikely that we will be able to observe (real) crystallization at the atomic level with such clarity soon, and therefore our simulations can provide experiment with insights into how such complex structures might evolve. In this

(30) Andersson, S.; Hyde, S. T.; Larsson, K.; Lidin, S. *Chem. Rev.* **1988**, *88*, 221−242.
(31) Anderson, M. W.; Egger, C. C.; Tiddy, G. J. T.; Casci, J. L.; Brakke, K. A. *Angew. Chem., Int. Ed.* **2005**, *44*, 3243−3248.
(32) Kresge, C. T.; Leonowicz, M. E.; Roth, W. J.; Vartuli, J. C.; Beck, J. S. *Nature* **1992**, *359*, 710−712.
(33) Davis, M. E. *Nature* **1993**, *364*, 391−393.
(34) do Carmo, M. P. *Differential Geometry of Curves and Surfaces*; Prentice Hall: Engelwood Cliffs, NJ, 1976.
(35) Hyde, S.; Andersson, S.; Larsson, K.; Blum, Z.; Landh, T.; Lidin, S.; Ninham, B. W. *The Language of Shape. The Role of Curvature in Condensed Matter: Physics, Chemistry and Biology*; Elsevier: Amsterdam, 1997.
(36) Gandy, P. J. F.; Klinowski, J. *Chem. Phys. Lett.* **2000**, *322*, 579−586.

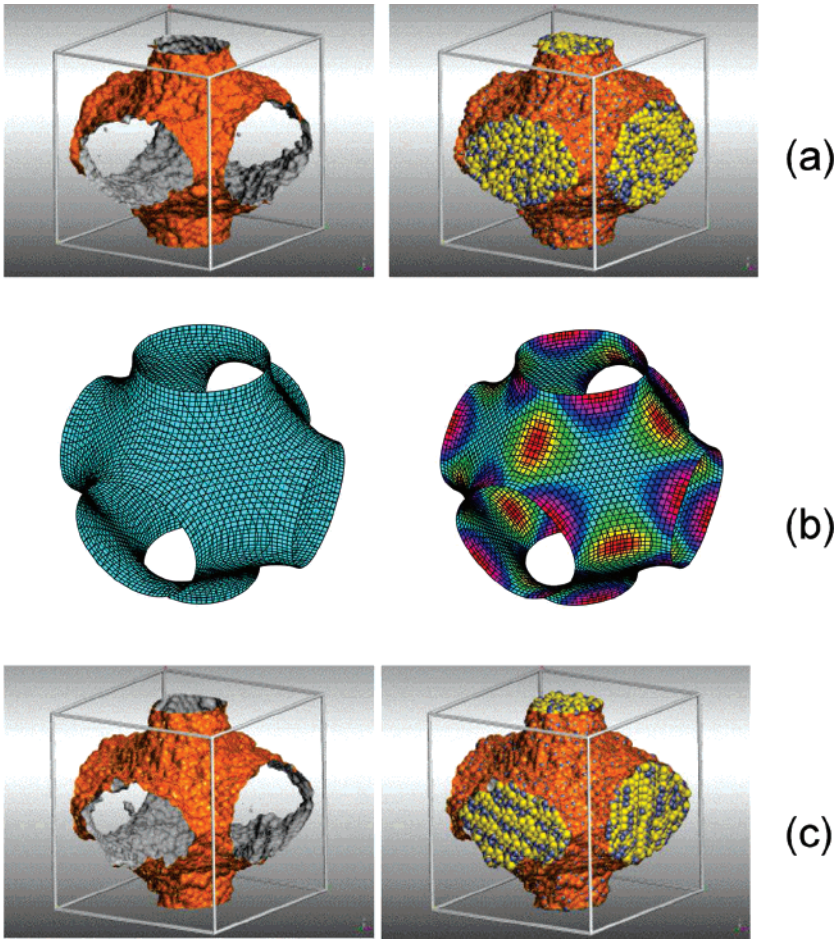

Figure 12. (a) Representation of the simulation cell corresponding to the 3D system comprising molten ZnS. (Left) surface rendered model; (right) surface rendered model and sphere model representations of the Zn (blue) and S (yellow) atom positions. (b) (Left) One unit cell (green) of the P minimal surface generated mathematically using the Weierstrass equation[34,36] rather than from atomistic models. (Right) A surface which differs from the true P surface (deviations from zero mean curvature is color coded from red to blue). (c) Same as (a) after crystallization and cooling.

case our simulations support the crystallization behavior proposed by Lu et al.

The amorphous frameworks crystallize into the wurtzite structure, a well-known polymorph of ZnS. In addition, we observe regions with hexagonal structures comprising mixed 4−8-membered rings. In conjunction with recent experimental and theoretical work, we propose that these crystal structures are intrinsically linked with the morphology and structure of the framework. Atomistic simulation and modeling techniques can therefore provide insights at the atomistic level into the surface structure of crystalline microporous materials.

The considerable curvature of the surface suggests that the surfaces are unlikely to exhibit similar chemical properties to the extended bulk surface of the parent material. Moreover, the chemistry is also likely to differ compared with similarly sized nanocrystals, because the curvatures of nanocrystals are typically convex compared with microporous framework structures, which are concave. Here, mathematical theories, pertaining to minimal surfaces, will help us to understand these structures. And in conjunction with quantum mechanical calculations, similar to extensive work and success on zeolites, we can probe the reactivity and shape−size selectivity of these internal cavities and channels.

Atomistic models, such as those presented here, are valuable as starting points to calculate, for example, physical and mechanical properties, sensitivity to temperature, catalytic activity at the surface of the channels or cavities (using quantum mechanical calculations), and electronic properties. The work presented here uses a framework simulation procedure for the generation of full atomistic models for mesoporous inorganic materials.

Acknowledgment. Cambridge-Cranfield HPCF, EPSRC (GR/S48431/1, GR/S48448/01, and GR/S84415/01).

Supporting Information Available: Movies depicting the crystallization, atomistic coordinates of mesoporous ZnS, and discussion of the ZnS crystal structure. This material is available free of charge via the Internet at http://pubs.acs.org.

JA0650697